

# Plasmon-coupled tip-enhanced near-field optical microscopy

A. BOUHELIER\*, J. RENGER†, M. R. BEVERSLUIS\* & L. NOVOTNY\*

\*The Institute of Optics, University of Rochester, Rochester, NY 14627, U.S.A.

†Technische Universität Dresden, Institut für Angewandte Photophysik, D-01062, Dresden, Germany

**Key words.** Field enhancement, scanning near-field optical microscopy, surface plasmons.

## Summary

Near the cut-off radius of a guided waveguide mode of a metal-coated glass fibre tip it is possible to couple radiation to surface plasmons propagating on the outside surface of the metal coating. These surface plasmons converge toward the apex of the tip and interfere constructively for particular polarization states of the initial waveguide mode. Calculations show that a radially polarized waveguide mode can create a strong field enhancement localized at the apex of the tip. The highly localized enhanced field forms a nanoscale optical near-field source.

## Introduction

Scanning near-field optical microscopy aims at optically resolving sub-wavelength structures. The most common technique relies on the local excitation of the sample surface by the optical fields near a nano-aperture in a metal overcoated glass fibre tip (Pohl *et al.*, 1984; Harootunian *et al.* 1986), alternatively, high-resolution fluorescence microscopy can also be achieved by using the local field enhancement produced at the end of a sharp metal tip when illuminated with the correct polarization state (Fischer, 1989; Sanchez *et al.*, 1999).

We propose a new method that does not require delicate technologies to produce nano-apertures (Veerman *et al.*, 1998; Bouhelier *et al.*, 2001), or the intense external focused beam responsible for field enhancement.

It has been suggested that surface plasmons can propagate on the surface of a metal-coated fibre tip (Keilmann, 1999). High-resolution fluorescence images were acquired using an opaque aluminium cantilever-based tip, suggesting the influence of a coupled mode in the metallic layer surrounding the quartz tip (Eckert *et al.*, 2000). A further step in the design of

plasmon-assisted microscopy can be found in Yatsui *et al.* (2002).

In this study, we show theoretical simulations that demonstrate that surface plasmons excited on the metal surface by a radially polarized propagating mode, also referred to as a radial doughnut mode, converge towards the very end of the tip where they interfere constructively and create a local excitation source.

## Description

Below the cut-off radius of an entirely metal-overcoated tapered optical fibre, modes are no longer guided. The large wavevectors associated with the electric fields after the cut-off can match the phase conditions for surface plasmons propagating on the outer side of the metal layer (Novotny *et al.* 1994). As a result, the electromagnetic energy associated with the initial waveguide mode can be coupled to the surface plasmons similar to the case of the well-known Kretschmann configuration applied to the excitation of surface plasmons on planar structures. After being excited, the surface plasmons propagate along the metal coating towards the tip apex. Because of the changing waveguide radius, the propagation of surface plasmons is accompanied by radiation losses which can be minimized by an adiabatically tapered tip. To create a strong field enhancement at the very end of the tip, the propagation of surface plasmons must interfere constructively. The condition of constructive interference is met only for certain symmetries and polarization states of the initial guided mode.

If a linearly polarized mode is injected into the fibre, the electric fields associated with the travelling surface plasmons cancel out at the end of the tip and hence do not provide any field enhancement (Fig. 1a). By contrast, if the mode inside the fibre is radially polarized, the rotational symmetry of the mode is such that the electric fields of the surface plasmons overlap in phase at the very end of the tip thereby producing a high surface charge density and thus a strong field enhancement (Fig. 1b).

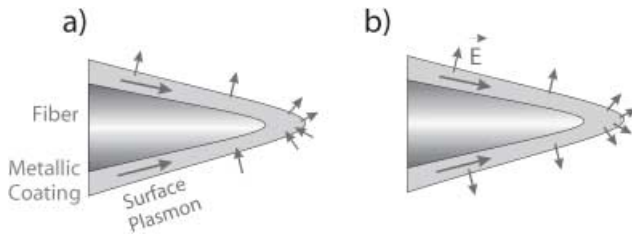


**Fig. 1.** Schematic of plasmons excited by (a) linearly polarized and (b) radially polarized propagating mode 0. In case (a) the electric fields cancel out at the very end of the tip preventing creation of a field enhancement, whereas in case (b) they interfere constructively and give rise to a field enhancement located at the end of the tip.

### Intensity distribution near the tip

The multiple multipole method (Hafner 1990) was applied to investigate the structure shown in Fig. 1. In the model, the fibre core has a dielectric constant of  $\epsilon_r = 2.18$  and a full cone angle of the taper of  $20^\circ$ . The fibre tip has a radius of curvature of 20 nm. A gold coating 70 nm thick overcoats the entire fibre tip and produces at the very end a cone-like metal particle with a radius of curvature of 5 nm. The dielectric function of gold at the excitation wavelength of 488 nm is  $\epsilon = -2.2 + i3.8$ .

We analysed the fields near the end of the tip for two different excitation symmetries. The first excitation source is a dipole located on the tip axis at the cut-off radius (2.38  $\mu\text{m}$  from the apex) and aligned perpendicular to it. This situation mimics the excitation with a linearly polarized fundamental  $\text{HE}_{11}$  waveguide mode. The azimuthal symmetries of dipole and  $\text{HE}_{11}$  mode are identical and are described by the functions  $\cos m\phi$  and  $\sin m\phi$ , with  $m = 1$  and with  $\phi$  being the polar angle with respect to the tip axis. The field of the dipole couples to  $m = 1$  waveguide modes and the latter couple to surface plasmons, which then propagate to the tip end. Because of the long distance between dipole and tip the field distribution near the tip end is influenced only slightly by the dipole's direct radiation field. Figure 2(a) shows a logarithmic plot (factor 2.33 between successive contour lines) of the resulting intensity distribution. The size of the image is  $2 \times 6 \mu\text{m}$ . The dashed line

in the figure represents the location of the dipole. Figure 2 demonstrates that surface modes are excited and that they converge towards the very end of the tip. Owing to the phase-mismatch introduced by the tapered geometry, surface plasmons couple weakly to far-field radiation which gives rise to a far-field background. The calculation also shows that there is no field enhancement produced at the end of the tip. Figure 2(b) shows a magnified view ( $120 \times 120 \text{ nm}$ ) and demonstrates that the polarization conditions give rise to a cancellation of the electric field at the end of the tip.

The second excitation source is a dipole situated at the same location as above but aligned parallel to the tip axis. This situation mimics the excitation with a radially polarized waveguide mode. The latter can be generated by the superposition of two perpendicularly polarized higher order modes. The azimuthal symmetries of dipole and radially polarized mode are identical and are described by azimuthal functions which are a constant ( $\cos m\phi$  with  $m = 0$ ). As before, we investigated the intensity distribution near the end of the gold-coated fibre tip using the same parameters. The dashed line in the figure represents the location of the dipole. Figure 3(a) shows that the dipole field couples to  $m = 0$  waveguide modes, which then couple to surface plasmons. Similar to the previous case, the surface plasmons propagate towards the tip apex. Besides the different intensity distribution inside the fibre, the main difference between the two configurations is the situation at the very end of the tip. Whereas in the previous situation the symmetry of the surface plasmons gave rise to a cancellation of the electric field at the end of the tip, this situation is characterized by a strongly enhanced field at the end of the tip (Fig. 3b). The enhancement originates from the fact that the phase relationship between the surface plasmons is such that the longitudinal field (field polarized along tip axis) adds constructively.

To determine favourable conditions for the field enhancement effect, we investigated the influence of the metal coating on the field enhancement. It is known that the excitation of surface plasmons on a flat surface is optimized for a certain thickness of the metal layer (Raether 1988). For the tip geometry the problem is less trivial. We investigated four different thicknesses of the gold layer and evaluated the field on a line transverse to the tip axis and 1 nm beneath the tip. The resulting

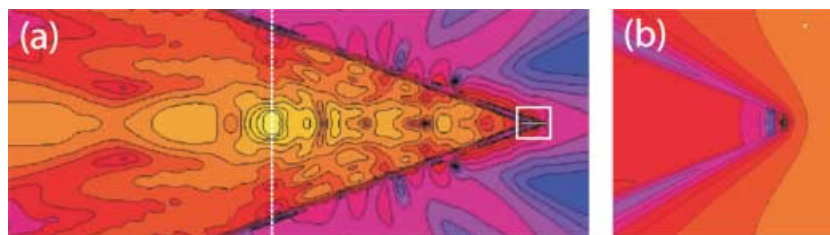


**Fig. 2.** (Left) Intensity distribution at the end of a gold-coated glass tip. An excitation dipole orientated perpendicular to the tip axis is placed at the cut-off radius as indicated by the dashed line (2.38  $\mu\text{m}$  from the apex) and shows no field confinement situated at the tip apex. Intensity plot with a logarithmic scale (factor of 2.33 between successive lines). Picture size is  $2 \times 6 \mu\text{m}$ . (Right) Magnified view of the very end of the fibre tip (factor of 1.62 between successive lines). Picture size is  $120 \times 120 \text{ nm}$ .

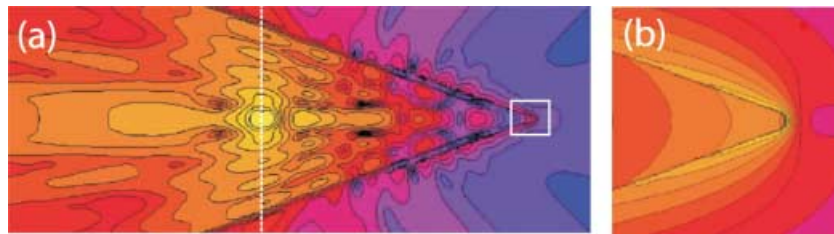


Fig. 3. (Left) Intensity distribution at the end of a gold-coated glass tip. An excitation dipole orientated along the tip axis at a location indicated by the dashed line. The polarization state is such that the requirements for creating a field enhancement are met. Intensity plot with a logarithmic scale (factor of 2.33 between successive lines). (Right) Magnified view of the very end of the fibre tip (factor of 1.62 between successive lines). Picture size is  $120 \times 120$  nm.

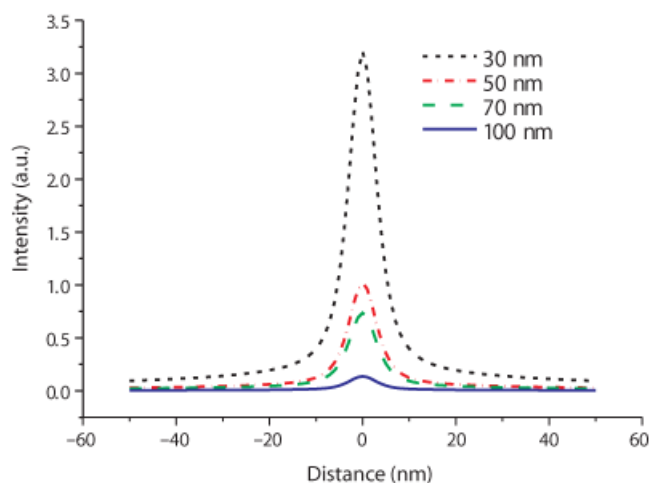


Fig. 4. Line scan 1 nm from the tip for different gold layer thicknesses. The background signal is due to radiative surface plasmons and finite transmission of the layer.

curves are shown in Fig. 4. We found that a thin layer of gold provides stronger field enhancement. However, the penetration through a thin layer is also stronger and hence a thin layer leads to a larger far-field background. By contrast, for a thick coating the penetration is much weaker leading to less far-field background, but also to much weaker field enhancement. We defined the relative enhancement factor  $f_e$  as the ratio between the intensity maximum in front of the tip and the background due to: (i) the finite transmission, and (ii) the radiatively decaying plasmon field. For the four thicknesses of 30, 50, 70 and 100 nm we obtain very similar values for  $f_e$  of  $\approx 35$ . Nevertheless, we conclude that an ideal film thickness is between 50 and 70 nm as it is experimentally difficult to coat homogeneously fibres with a film thickness  $< 50$  nm. It should be emphasized that the field confinement is independent of the coating thickness. Figure 5 shows the full-width at half-maximum (FWHM) of the line scans in Fig. 4 vs. the coating thickness. The confinement of the field stays constant at roughly the end diameter of the tip, suggesting that the

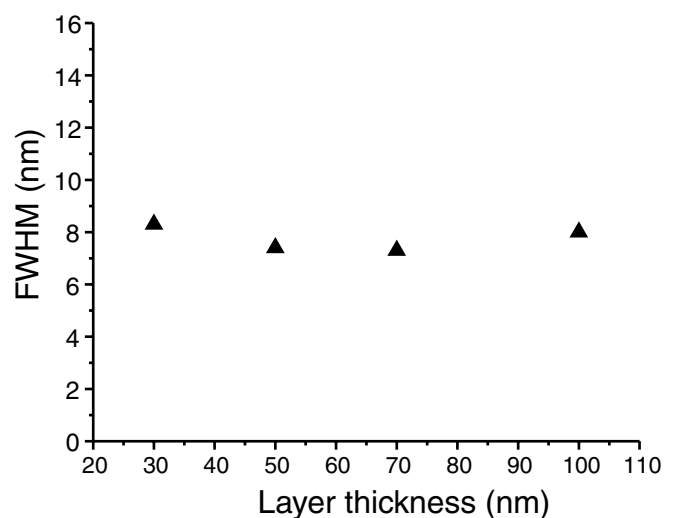


Fig. 5. Full-width at half-maximum of the intensity confinement for four different gold layer thicknesses. The confinement of the field stays constant and is mainly given by the diameter of the tip apex.

resolution that can be achieved with these tips is given by their sharpness.

#### Waveguide modes excited by a dipole outside the probe

To confirm that excitation by a radially polarized mode provides the optimum conditions for strong field enhancement, we investigated the reciprocal problem. A dipole was placed at the very end of the tip on the vacuum side. The dipole was orientated along the symmetry axis. Figure 6 shows the resulting field distribution. Because the dipole is orientated along the tip axis, the coupling between tip and dipole is rather weak and most of the energy is radiated to the sides. A small fraction of the dipole's energy couples to the tip and is converted to propagating radiation inside the metal-coated fibre. Figure 7 shows the distribution of the transverse field ( $E_x^2$  and  $E_y^2$ ) on a plane perpendicular to the tip axis at a distance of  $2.38 \mu\text{m}$  from the apex. This distance is just beyond

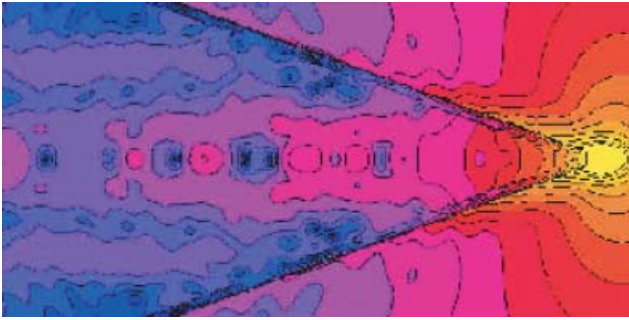


Fig. 6. Coupling between the metal-coated fibre and a dipole situated at the apex of the fibre. Weak coupling is observed due to the orientation of the dipole. A propagating mode is also forming inside the core of the fibre. Intensity plot with a logarithmic scale (factor of 2.33 between successive lines).

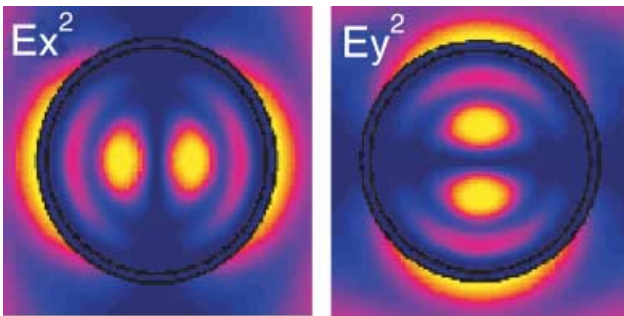


Fig. 7. Cross-sections of the transverse fields  $E_x^2$  and  $E_y^2$  at the cut-off radius for a dipole excitation outside the fibre. The patterns resemble two Hermite–Gaussian (1,0) modes with orthogonal polarizations. The combination of these two modes creates a radially polarized beam.

the cut-off radius. The images seen in Fig. 7 resemble two Hermite–Gaussian (1,0) modes with orthogonal polarizations. The superposition of these modes creates a radially polarized mode (Novotny *et al.* 1998). Thus, the field distribution is a ring and polarization is radial. This confirms that a radially polarized mode is the favourable mode for creating an enhanced and localized field near the tip apex.

### Propagation of radially polarized fibre modes

The fundamental modes propagating inside a waveguide with a circular cross-section such as an optical fibre are the analogous TE and TM modes propagating inside a rectangular waveguide. Whereas the TE mode has an azimuthally polarized electric field, the TM mode has a radially polarized field (Jackson 1998). These particular modes are decoupled only if there are no azimuthal variations of the fields, which makes them very sensitive to the quality of the injection, as well as to outside vibrations. If longitudinal fields are nonzero, the modes are no longer transverse but hybrids.

Figure 6(a) shows experimental intensity distributions of such a hybrid mode after it has been coupled out from a

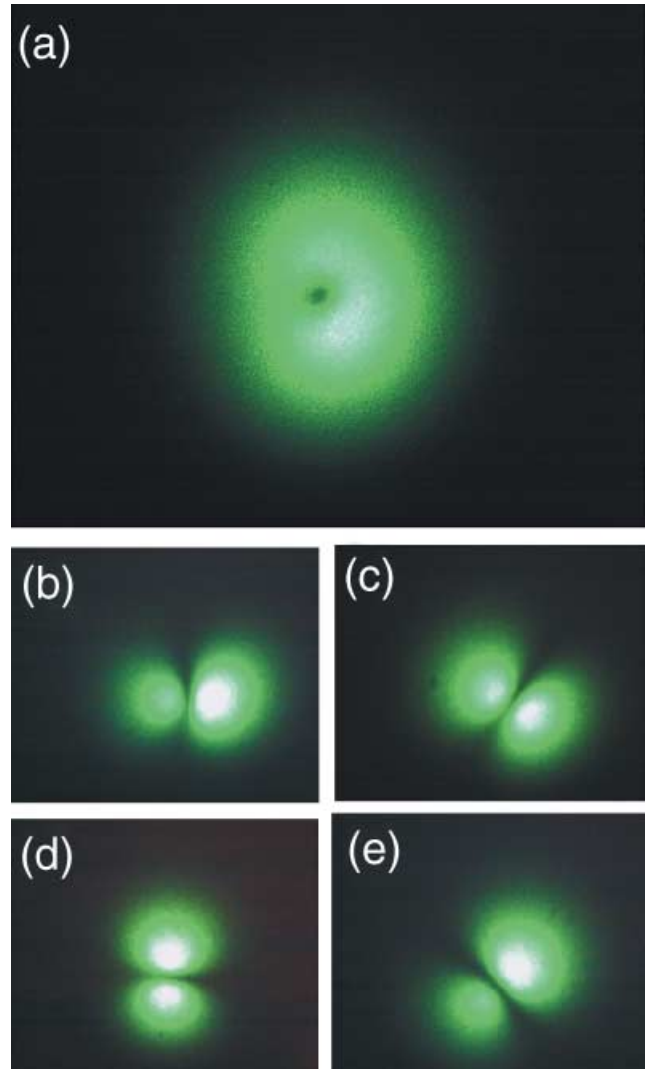


Fig. 8. (a) Radially polarized mode coupled out from a fibre. (b–e) Polarization characteristics of the mode. (b) Mode polarization state after analyser orientated at  $0^\circ$ , (c) at  $+45^\circ$ , (d) at  $+90^\circ$  and (e) at  $-45^\circ$ .

cleaved fibre and projected on a screen. The fibre is designed to support only a single mode at  $\lambda = 632$  nm. Because we need to excite a higher order mode we chose a shorter wavelength ( $\lambda = 532$  nm). Before sending the laser beam into the fibre we performed a mode conversion using bisected phase plates (Quabis *et al.* 2000, 2001). This mode conversion creates a multitude of modes, but the subsequent spatial filtering by the fibre suppresses all high-order modes. Figure 8 shows that the radially polarized symmetry of the modes is preserved after propagating through the fibre. The state of polarization was tested by using a polarizer placed at the end of the fibre. Figure 8(b–e) depict situations in which the polarizer direction was orientated at  $0$ ,  $+45$ ,  $+90$  and  $-45^\circ$ . Despite some slight asymmetries of the mode, the radial characteristics of the electric field are well maintained. It should be emphasized

that such a mode is not easily coupled to the fibre and its polarization depends strongly on the quality of the injection and on the mechanical stress (bending) applied to the fibre.

### Conclusions

Our theoretical simulations show that a radially polarized excitation mode is needed to establish a strong field enhancement at the end of an entirely gold-overcoated fibre tip. Near the cut-off radius, the field of the exciting mode couples to surface plasmons that propagate on the outside surface of the metal coating. The excited surface plasmons propagate towards the tip end. The symmetry of the radial excitation beam ensures that a strong field enhancement is created at the metallic tip. We showed that radially polarized modes can propagate in optical fibres and that they can be used for subsequent excitation of a tapered near-field geometry.

### Acknowledgements

The authors wish to thank J.-J. Greffet, B. Hecht and L. Eng for helpful discussions. This research was funded partially by the Swiss National Foundation (AB) and by NSF grant No. DMR-0078939.

### References

- Bouhelier, A., Toquant, J., Tamaru, H.G., Güntherodt, H.-J., Pohl, D.W. & Schider, G. (2001) Electrolytic formation of nano-apertures for scanning near-field optical microscopy. *Appl. Phys. Lett.* **79**, 683.
- Eckert, R., Freyland, J.M., Gersen, H., Heinzelmann, H., Schurmann, G., Noell, W., Staufer, U. & de Rooij, N. (2000) Near-field fluorescence imaging with 32 nm resolution based on microfabricated cantilever probes. *Appl. Phys. Lett.* **77**, 3695.
- Fischer, U.C. (1989) Resolution and contrast generation in scanning near-field optical microscopy. *Scanning Tunneling Microscopy and Related Methods. NATOASI Series, Vol. 184* (ed. by R. J. Behm, N. Garcia and H. Rohrer). Kluwer, Dordrecht.
- Hafner, C. (1990) *The Generalized Multiple Multipole Technique for Computational Electromagnetics*. Artech, Boston.
- Harootunian, A., Betzig, E., Isaacson, M. & Lewis, A. (1986) Super-resolution fluorescence near-field scanning optical microscopy. *Appl. Phys. Lett.* **49**, 64.
- Jackson, J. (1998) *Classical Electrodynamics*. Wiley, New York.
- Keilmann, F. (1999) Surface-polariton propagation for scanning near-field optical microscopy. *J. Microsc.*, **194**, 567.
- Novotny, L., Pohl, D.W. & Regli, P. (1994) Light propagation through nanometer-sized structures: the two-dimensional-aperture scanning near-field optical microscope. *J. Opt. Soc. Am. A*, **11**, 1768.
- Novotny, L., Sanchez, E.J. & Xie, X.S. (1998) Near-field optical imaging using metal tips illuminated by higher-order hermite-gaussian beams. *Ultramicroscopy*, **71**, 21.
- Pohl, D.W., Denk, W. & Lanz, M. (1984) Optical stethoscopy: image recording with resolution  $\lambda/20$ . *Appl. Phys. Lett.* **44**, 651.
- Quabis, S., Dorn, R., Glockl, O., Eberler, M. & Leuchs, G. (2000) Focusing light to a tighter spot. *Opt. Commun.* **179**, 1.
- Quabis, S., Dorn, R., Glockl, O., Reichle, M. & Eberler, M. (2001) Reduction of the spot size by using a radially polarized laser beam. *Proc. SPIE* **4429**, 105.
- Raether, H. (1988) *Surface Plasmons. Springer Tracts in Modern Physics III*. Springer-Verlag, Berlin.
- Sanchez, E.J., Novotny, L. & Xie, X.S. (1999) Near-field fluorescence microscopy based on two-photon excitation with metal tips. *Phys. Rev. Lett.* **82**, 4014.
- Veerman, J.A., Kuipers, A.M.O. & Hulst, N.F. (1998) High definition aperture probes for near-field optical microscopy fabricated by focused ion beam milling. *Appl. Phys. Lett.* **72**, 3115.
- Yatsui, T., Itsumi, K., Kourogi, M. & Ohtsu, M. (2002) Metallized pyramidal silicon probe with extremely high throughput and resolution capability for near-field technology. *Appl. Phys. Lett.* **80**, 2257.